Sources of imprecision in the determination of lateral energy fraction and perceptual investigations

Bachelorarbeit aus Aufnahmetechnik 1, SE

Seo Jiwon
Zagala Franck

Betreuung: Dr. Alois Sontacchi

Graz, July 30, 2015

institut für elektronische musik und akustik

Abstract

The early lateral energy fraction (LF) is one of the most important room acoustic parameters for apparent source width (ASW). However, the measurement of LF suffers from many imprecisions and then represents incongruity. To investigate how various parameters affect LF, diverse rooms were generated by means of ambisonics on a loudspeaker-array and LFs were measured by two different microphone systems with a variation of conditions. Diverse factors describing the microphones and their use were investigated and a calibration between an omni-directional and figure-of-eight microphones was performed thereafter. Another alternative with tetrahedral microphone-array was examined and compared to the conventional method. The fluctuations of LF were also taken into account to improve the precision of the measures and its suitability in an ASW evaluation context. The appropriateness between the values of LF and auditory perceptions was then demonstrated with a simple psycho-acoustical test.

Acknowledgements

We would like to thank Dr. Sontacchi for his great supervision and support in this work.

Many thanks to Dr. Kahle for his great suggestions and help.

We are very grateful to all the staff of IEM, who played a significant role, directly or indirectly, in the realisation of this work.

Finally we are thankful to all the participants of the listening-test.

Contents

1 Introduction

1.1 Spatial impression

In a room acoustic environment, like a concert hall or an opera house, the spatial impression is a vital factor to evaluate the quality of the hall. When attending a musical performance in a hall, the sense of spaciousness gives listeners the impression of depth and width, the feeling to be enveloped by sound and then the satisfaction of listening as a result.

There have been many studies about this concept over the last decades. For the first time, *Beranek* found in 1962 that the reflections arriving after the direct sound within 60ms enhance the texture of music, that is to say, improve the intimacy as if the music was played in a small room [Ber62]. Hence he introduced *initial-time-delay-gap* that means the time difference between arrival of the direct sound and the first reflection. Following researches concluded that among the early reflections, those from lateral directions are crucial for the sensation of spatial impression [Mar67, Mar68, Bar71, TH95].

According to a general classification, the spatial impression results primarily from two subcomponents:

The first one is *Apparent Source Width (ASW)*, defined at first by *Barron and Marshall* in [BM81], which refers to the width of sound image caused by the lateral reflections. Two acoustic parameters, the *Inter-Aural Cross-correlation Coefficient (IACC)* and *Early Lateral Energy Fraction (LF)*, are the most important quantitative parameters to be representative of the ASW. The IACC is derived from the correlation between both channels of binaural impulse responses. The LF defined first in [BM81], as the main topic in this work, will be explained in detail shortly.

The second one, introduced in [JB95a, JB95b], is *Listener Envelopment (LEV)* defined as the degree of fullness of sound images around a listener, in other words, the sensation that the listener is enveloped by the sound field. The representative acoustical parameter of LEV is *Late Lateral Energy Level (GLL)*. This is strongly related to the level of the late lateral sound energy (later than 80ms). In figure 1, these two subcomponents are shown graphically.

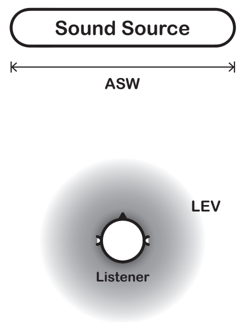

Figure 1 – Apparent Source Width and Listener Envelopment

In the present study, we mainly focus on LF and its derived perception parameter ASW.

1.2 Lateral energy fraction

The (early) lateral energy fraction describes the ratio of the sound energy measured by a figure-of-eight microphone to the sound energy measured by an omni-directional microphone, within 80 ms. According to ISO3382 [ISO09], the early lateral energy fraction is defined as in the following :

$$\mathrm{LF} = \frac{\int_{0.005}^{0.080} p_{\infty}^2(t)dt}{\int_{0.000}^{0.080} p_{\circ}^2(t)dt,} \tag{1}$$

where $p_{\infty}(t)$ is a sound pressure measured by the figure-of-eight microphone and $p_{\circ}(t)$ is that measured by the omni-directional microphone. The microphones have to be placed at the same position. The zero-direction of the figure-of-eight microphone is oriented to the sound source. *"As a higher delay limit the figure of 80 ms is proposed. Although reflections of delays greater than 80 ms produce a spatial effect, 80 ms corresponds roughly to the area of transition between the effects of early reflections and those of reverberation. The limit of 80 ms also corresponds roughly with the time limit after which discrete reflections can become disturbing with music" [BM81] S.230.* The bottom time-boundary in the numerator (5ms) is here to get rid of the direct sound into the figure-of-eight microphone.

LF can also be expressed in a different way:

$$\mathrm{LF} = \frac{\int_{0.005}^{0.080} p_{\circ}^2(t)\cos^2(\phi)dt}{\int_{0.000}^{0.080} p_{\circ}^2(t)dt,} \tag{2}$$

The angle ϕ means here the azimuthal angle between the direction of a sound wave and the microphone axis. The position and orientation of two microphones for measuring the LF are represented graphically in figure 2, showing the azimuthal angle ϕ.

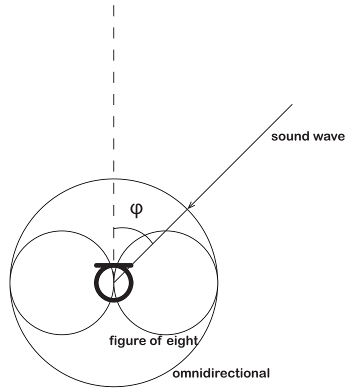

Figure 2 – Position and orientation of the two microphones

1.3 Outlines of the present study

In this work we focus on the parameter LF.

This document consists of four chapters.

First of all, we investigate how various factors affect the measurement of LF, such as spacing or orientation in the practical situation as well as the characteristics of microphones. Then a calibration between a figure-of-eight and an omni-directional microphone is carried out.

As a next step, we consider a measurement method using a Soundfield microphone. Here we face problems caused by a geometrical limitation and hence examine the appropriateness of the method.

In the third chapter, spatial fluctuations, resulting from an interference phenomenon in a sound field, is considered. By increasing measurement positions and averaging the values, it is observed that a more corresponding result is obtained.

Finally in the last chapter, by conducting a listening experiment with several subjects, measurement values are compared with listeners perceptions.

2 Experimental setup

In order to investigate the behavior of LF-values in diverse room environments with a variation of conditions, such as measurement positions and delay-times of reflections and to present how it is actually perceived, an experimental measurement was undertaken.
All measurements were conducted in IEM CUBE which has a hemisphere of 24 loudspeakers.

Figure 3 – CUBE IEM - University of Music and Performing Arts, Graz - Alexandre Castonguay

2.1 Room simulations

In order to create diverse acoustical environments, a direct sound and four early artificial reflections were created with the help of 4th order Ambisonics in *Pure Data*. The angles of incidence of these four reflections were varied in order to obtain 5 ”rooms” with potentially different LF-values (see figure 4).

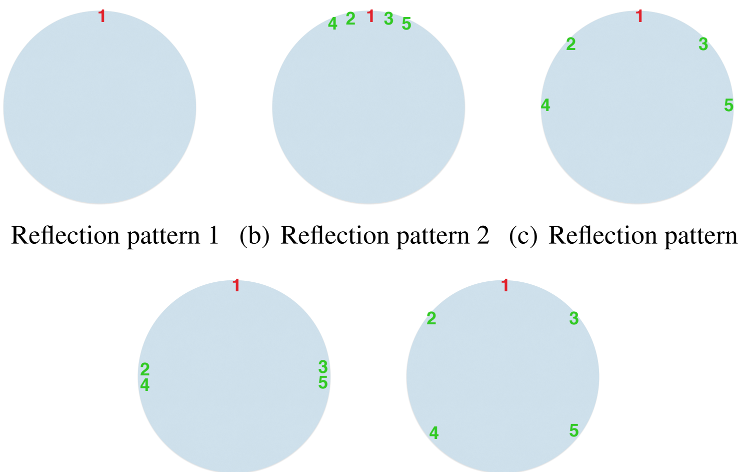

(a) Reflection pattern 1 (b) Reflection pattern 2 (c) Reflection pattern 3

(d) Reflection pattern 4 (e) Reflection pattern 5

Figure 4 – Reflection patterns generated by Ambisonics in CUBE

Number 1 (red) in the figures indicates the direct sound and the numbers from 2 to 5 (green) represent the generated early reflections.

Room 1 does not contain any artificial reflections but only a direct sound and the natural reflections of the IEM CUBE.
Four reflections were added to the other rooms.
Room 2 has its generated reflections near the direct sound.
Room 3 has evenly spread reflections from the front direction.
Room 4 represents an extreme case in which all reflections come from the both sides.
Room 5 has evenly distributed reflections, from the rear as well as from the front.
The elevation of the reflections and direct sound are intentionally set to $0°$. The gains and delays of the reflections are shown in table 1. The gain of the reflections remained -3dB and two different versions of delay-time were measured (here named ”Delay 1” and ”Delay 2”). For left and right side a different delay-time was created to avoid extreme interferences in the sound field caused by the geometrical symmetry.

	meas. 1		meas. 2	
room	delay	gain	delay	gain
1	0ms	0dB	0ms	0dB
2	8ms	-3dB	27ms	-3dB
3	10ms	-3dB	30ms	-3dB
4	18ms	-3dB	57ms	-3dB
5	20ms	-3dB	60ms	-3dB

Table 1 – Delays and gains of the generated reflections

2.2 Procedure of measurement

In figure 5, the flow-diagram of the measurement setup is shown.

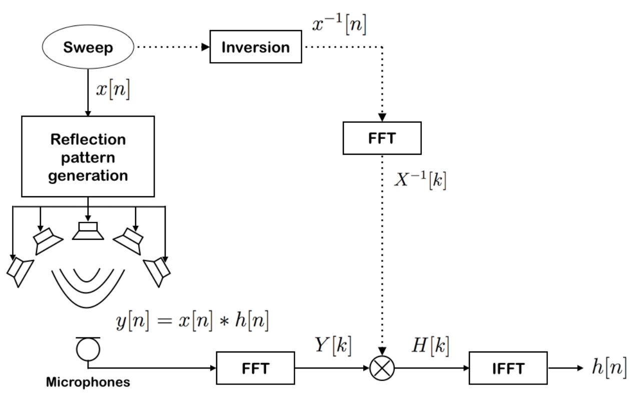

Figure 5 – Flow-diagram of measurement setup

The impulse response was calculated with a three seconds exponential sweep from 60Hz to 20kHz. The impulse response was obtained with a fast-convolution between the system response and the inverse sweep. In the measurement, microphones were located in the center of the room (position E) and at two additional positions on each side, with an offset of 7cm (see positions A and B reffig:cube).

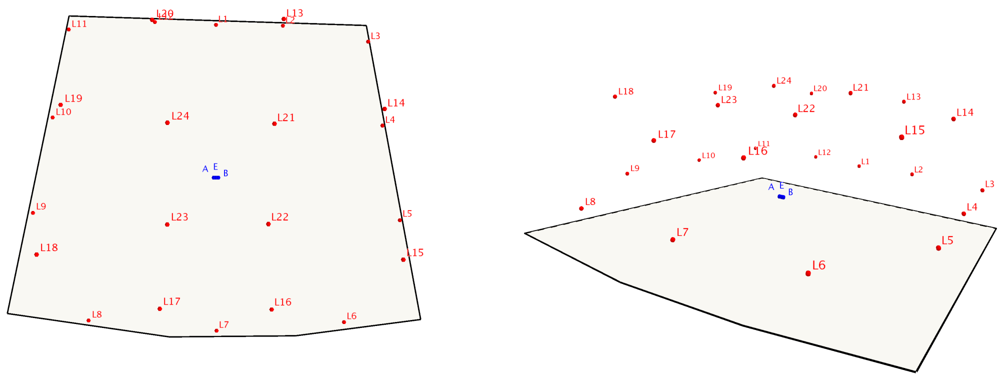

Figure 6 – Geometry of IEM-CUBE

2.3 Measurement equipment

Several microphones were used in the measurement: an omni-directional microphone *Schoeps MK2* which is for free field placement, a figure-of-eight microphone *Schoeps MK8* and a tetrahedral microphone array *Soundfield SPS200* and an artificial head *Brüel & Kjaer*. All microphones were placed at a height of 1.25m over the floor. Although [ISO09] suggests the use of a diffuse-field microphone for diaphragm diameter greater than 16mm, the use of spectral correction between the MK2 and MK8 allowed us the use of a free-field microphone (see chapter 3.2).

3 Uncertainty of measurement

This chapter deals with several factors which result in uncertainty of the measured LF-values and a calibration between an omni-directional and a figure-of-eight microphone.
Five factors were introduced and analysed: Polar-pattern of microphones, orientation, spacing, gain and spectrum.
The calibration was implemented by two different methods: an energetic interpolation for each octave-band and a spectral division between two channels.

3.1 Influential factors to LF

3.1.1 Polar-pattern of microphones

In practical situations, the polar pattern of microphones used for measuring the LF does not keep the ideal state but rather gets distorted in some degree.
In [Beh03], a simulation to determine the impact of the microphone directivity pattern was undertaken. To determine the LF values the impulse response was calculated with ray-tracing in a room of dimensions $15\text{m}\times15\text{m}\times21\text{m}$. Thus the influence of different polar-pattern parameters were investigated, such as the exponent of figure-of-eight, tendency of omni-directional to ideal cardioid and asymmetry of the figure-of-eight. The results are given in figure 7.

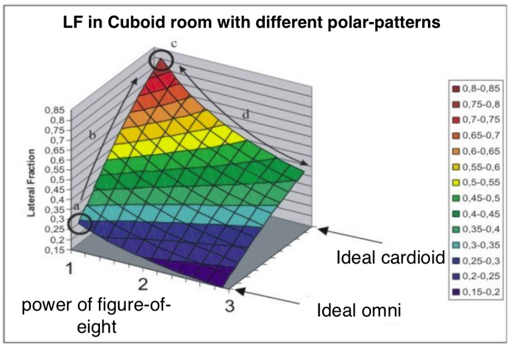

(a) Influence of exponent of figure-of-eight and ratio omni/cardioid

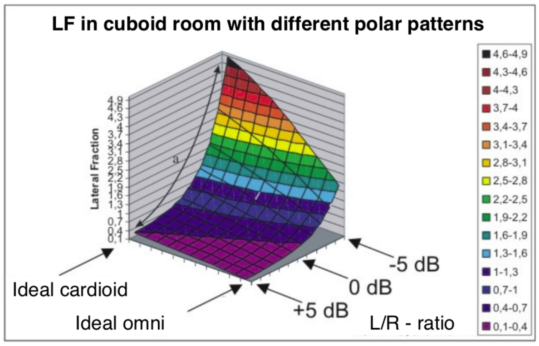

(b) Influence of ratio omni/cardioid and asymmetry of figure-of-eight

Figure 7 – Influence of various polar pattern parameters on LF (cuboid room)

This results were compared to a simulation concerning a concert room with a "more complex geometry" and it appeared that the trends of the curves are highly similar. However, some differences were observed: with identical variations of the polar-pattern characteristics, the range of LF is smaller in the concert hall than that in the case of the cuboid room. With ideal figure-of-eight and changing the omni to cardioid, the LF-values go from 0.3 to about 0.85 in the cuboid room while merely 0.5 is obtained in the concert hall.
In conclusion the influence of the pickup pattern depends on the sound field.

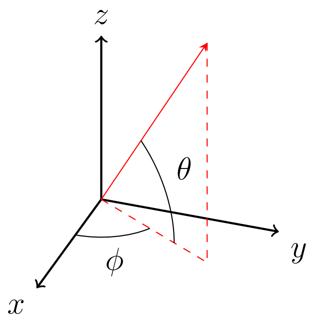

Figure 8 – Spherical coordinates

3.1.2 Orientation

In practical situation it might be difficult to orientate precisely the figure-of-eight microphone toward the source. For this reason, the influence of orientation was investigated by employing B-format.
In order to investigate this influence, an experiment was conducted with a Soundfield microphone. Any orientation of a figure-of-eight channel can easily be generated as a linear combination of the the channels X,Y and Z. The following expressions represent the B-format components up to first order in spherical coordinates (see Figure 8).

$$W = S \cdot \frac{1}{\sqrt{2}} \tag{3}$$
$$X = S \cdot \cos\theta \cos\phi \tag{4}$$
$$Y = S \cdot \sin\theta \cos\phi \tag{5}$$
$$Z = S \cdot \sin\phi \tag{6}$$

Thus, in order to rotate the figure-of eight channel horizontally, X and Y are weighted with coefficients with respect of θ. The Y-component which is warped as much as x degree, is represented as following :

$$Y = \sin(\theta + x) \cdot \cos\phi = \mathsf{a} \cdot \cos\theta \cos\phi + \mathsf{b} \cdot \sin\theta \cos\phi \tag{7}$$
$$\sin(\theta + x) = \mathsf{a} \cdot \cos\theta + \mathsf{b} \cdot \sin\theta, \tag{8}$$

where $a = \sin x$ and $b = \cos x$. On the basis of this theoretical explanation, our experiment yielded corresponding LF-values in five rooms (see Appendix B).

Figure 9 shows the LF-values as a function of an angle in the five rooms. The angle indicates the difference between the actual orientation of figure-of-eight during the measurement and the simulated orientation of the figure-of-eight. Up to 15°, the deviation stays within 1 JND (0.05 [TJC93]) in all rooms. The noticeable results are observed in room 2 and 4. In room 2, the reflections are very close to the direct sound and a significant difference of the LF-value appears from 30°, viz. LF-values increase considerably.

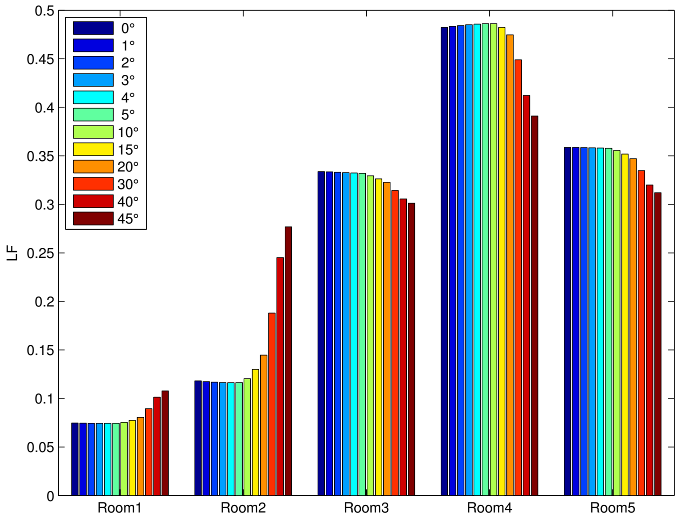

Figure 9 – LF depending on orientation mistakes

In room 4, the reflections come from nearly 90° on the side, hence LF-values decrease at large twisted angles. Considering that rooms 2 and 4 are extreme cases and assuming a measurement in a concert hall with a complex geometry, we arrive at a conclusion that the orientation error has little influence on the LF, up to some degree.

3.1.3 Spacing

In [MCVS13] Vigeant *et al.* conducted an experiment to investigate the effect of spacing between the figure-of-eight and the omni-directional microphone when measuring the LF. In their measurement setup, two distances, 89 mm and 152 mm respectively, were tested by measuring the LF with eight diverse microphones at two measurement positions. Statistically, ΔLF is equal to 0.023 at position R1 and 0.013 at position R2 and the standard deviation is 0.024 at position R1 and 0.015 at position R2 (see figure 10) . All values from each microphone lie within 1 JND (the JND-value was assumed as 0.05 in their work). Therefore the authors concluded that the effect of spacing on LF is negligible.

3.1.4 Gain and spectrum

The importance of the gain-calibration between the figure-of-eight and omni-directional channels is considerable, since the energetic gain of each signal directly affects the value of LF. In other words, a gain of +3dB on the figure-of-eight would double the LF-value.

$$\mathrm{LF}_2 = \frac{\int_{0.005}^{0.080} (\alpha \cdot p)_\infty^2(t)dt}{\int_{0.000}^{0.080} p_\circ^2(t)dt} = \alpha^2 \cdot \mathrm{LF}_1 \tag{9}$$

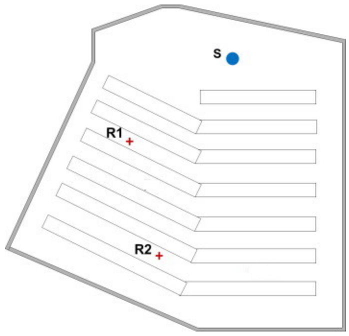

Figure 10 – Measurement positions in the experiment for spacing [MCVS13]

Spectrum discordance between the omni-directional and the figure-of-eight microphone leads also to uncertainty of LF. The fundamental cause of the spectrum discordance is structural difference between these two types of microphones: respectively sound pressure and sound pressure gradient. The sound pressure microphone keeps relatively a quite flat spectrum over whole frequency domain, on the contrary, the gradient microphone suffers from a decline of the sensitivity for low frequencies due to the phase change across space.
Figure 11 shows the disagreement of LF-values without and with calibration (see spectral correction, chapter 3.2).

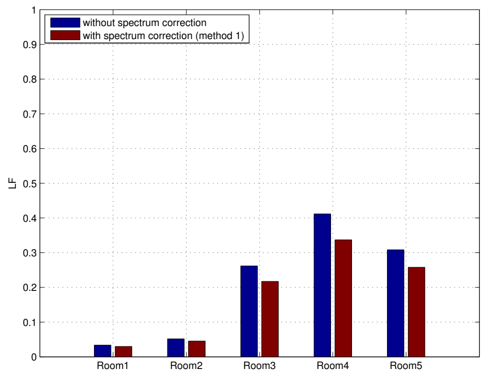

Figure 11 – LF without and with calibration (spectral correction)

For each room, there is a noticeable difference between the original and calibrated LF-value, that is to say, 1.5 JND in room 4. For this reason it is recommended to calibrate the spectrum of both microphones together.

3.2 Calibration of a pair of microphones

To avoid the imprecision generated by the gain and spectrum differences between the two channels, a calibration was undertaken to achieve the spectrum coincidence of both microphones.

First, a calibration measurement was carried out with a short distance of 1.2m between the loudspeaker and the microphones in order to increase the time-interval between the direct sound and the first reflections from the floor and not too close in order to avoid the proximity effect with the figure-of-eight.
Two methods were employed to create a correction spectrum:

1. Both signals were filtered by octave filters of order 3 according to ANSI S1.1-1986 standard with center frequencies from 31.5 to 8kHz, the energy of the first 220 samples @44100Hz (just before the first reflection) was then calculated for each channel. The ratio between the energy of the omni-directional and the figure-of-eight microphone for each octave-band determined a spectral correction factor. These factors were then interpolated (piecewise cubic interpolation) over the whole frequency-range (see figure 12(a) and Appendix C).
2. The amplitude spectrum of the correcting filter was also determined with a spectral division of both microphones (see figure 12(b) and Appendix D).

From these amplitude spectrums, a minimum-phase filter can be created this way:

— Symmetrisation of the interpolated correcting spectrum at Nyqvist frequency
— Computation of cepstrum
— Windowing in cepstral domain (convolution with analytical signal in time domain)
— Converting to inverse cepstrum to obtain the impulse response of the minimum phase correction filter

The procedures corresponding to two methods are explained graphically in figure 12.
y_m presents the impulse response of the minimum-phase filter.

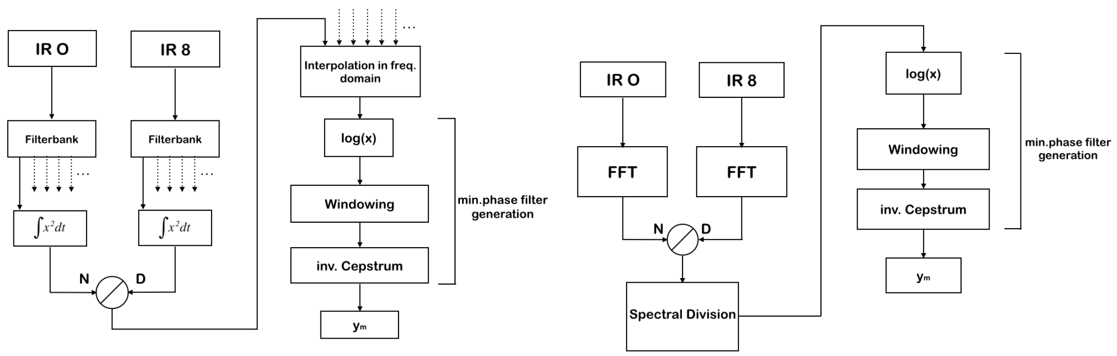

(a) Method 1 (b) Method 2

Figure 12 – Flow diagram of the two calibration methods

After a convolution between all signals from the figure-of-eight and the impulse response of the minimum-phase filter, both microphones are assumed to be calibrated.

In the calibration method 2, some distortions could be observed in the spectrum, this may be the result of the spectral division between very small values. For this reason it appears that this calibration method might not be optimal. On the other hand, the

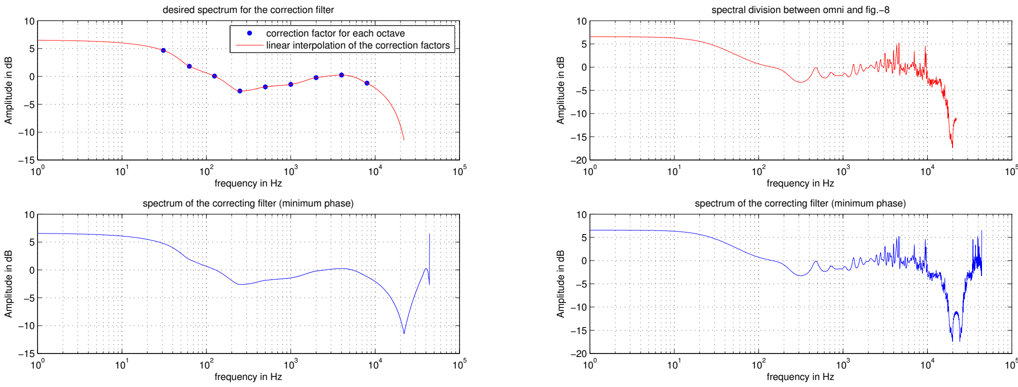

(a) Method 1 (b) Method 2

Figure 13 – Design of minimum-phase correction filter

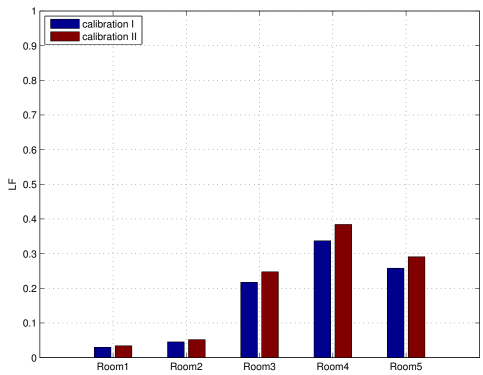

Figure 14 – LF with calibration method 1 and 2 (position E)

calibration method 1, based on an energetic cubic interpolation of each octave, appears much smoother and does not suffer from such division problems of small values.
Because of the above mentioned distortion in spectrum, the value of LF might be affected, as shown in figure 14.

4 Measurement with Soundfield microphone

For measuring of 3D impulse responses in a sound field, spherical microphone-arrays have been used since this microphone concept was developed. So it made sense to use a tetrahedral microphone to measure lateral energy fraction. This chapter reports the measurement when using a Soundfield microphone.

4.1 Introduction to ambisonics and B-format

Ambisonics is an approximated sound field representation. The pressure at a point $\mathbf{r}$ can be described as following [Bat09]:

$$p(\mathbf{r}, k) = \sum_{n=0}^{n=\infty} \sum_{m=-n}^{m=n} A_n^m(k) J_n(kr) Y_n^m(\theta, \phi), \tag{10}$$

where $A_m^n(k)$ are ambisonics coefficients, J_n the Bessel function of the first kind and Y_n^m describes the spherical harmonics:

$$Y_n^m(\theta, \phi) = \sqrt{\frac{2n+1}{4\pi} \frac{(n-m)!}{(n+m)!}} P_n^m(cos\theta) e^{jm\theta}, \tag{11}$$

P_n^m is the Legendre-Polynom. n is order and m is degree
Figure 15 shows the spherical harmonics up to third order.

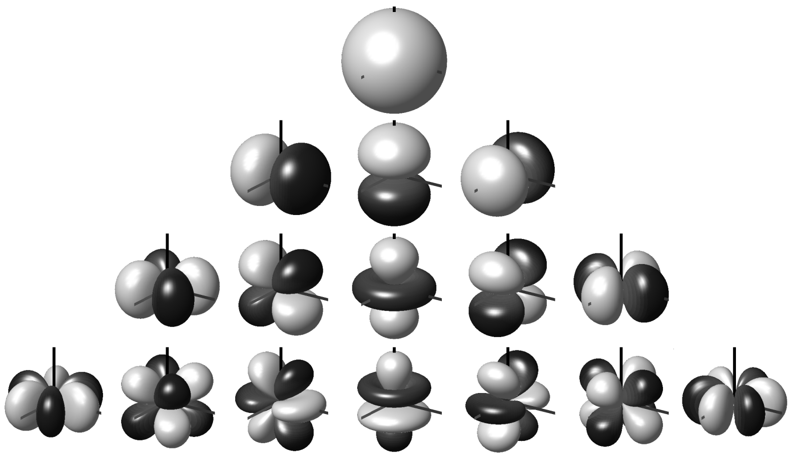

Figure 15 – Spherical harmonics [Amb]

In the case of a tetrahedral microphone array, four cardioid capsules are spread on the edges of a tetrahedron. The geometrical description of SPS200 is given in table 2 and figure 16.

Capsule	Azimuth	Elevation
LFU	$45°$	$35,2644°$
RFD	$315°$	$-35,2644°$
LBD	$135°$	$-35,2644°$
RBU	$225°$	$35,2644°$

Table 2 – Coordinates of the capsules (Soundfield microphone SPS200)

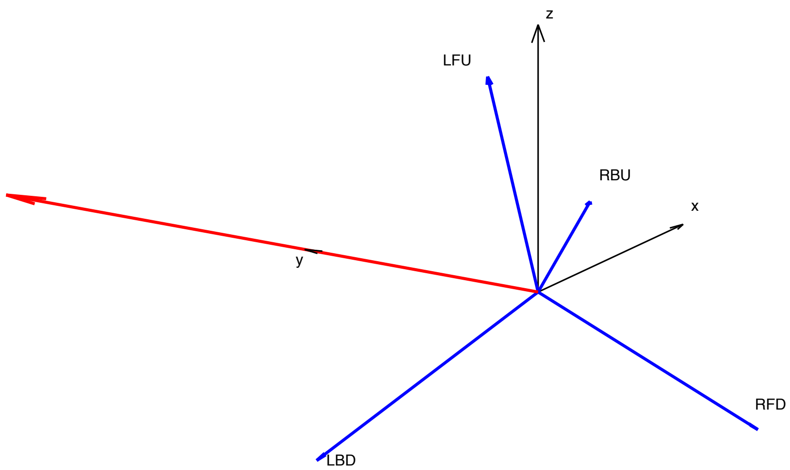

Figure 16 – Vectorial representation of the A-format and Y-channel of the B-format

The original signals from the capsules is called *A-format*, these signals can be easily converted into *B-format* of first order where each channel corresponds to a spherical harmonic. The equations from 12 to 15 represent the conversion formulas (encoding).

$$W = LFU + RFD + LBD + RBU \tag{12}$$
$$X = LFU + RFD - LBD - RBU \tag{13}$$
$$Y = LFU - RFD + LBD - RBU \tag{14}$$
$$Z = LFU - RFD - LBD + RBU \tag{15}$$

The W signal corresponds to an omni-directional microphone, whereas X, Y and Z are the components that would be picked up by figure-of-eight capsules oriented along the three spatial axes [Amb].

4.2 Calibration in B-format

As described in equation 3, the W-component has to be attenuated theoretically by 3dB, so that it contains the same energy as the other channels [Amb]. Supposing all capsules identical, a great advantage of measurements with Soundfield microphone over the conventional method is that it does not require a spectral calibration (at least for low frequencies).

4.3 Polar pattern distortion in B-format

The soundfield microphone SPS200 consists of four sub-cardioid capsules. The following figure 17 shows the polar-pattern of the capsules of a different Soundfield microphone, namely the *DSF-1*.

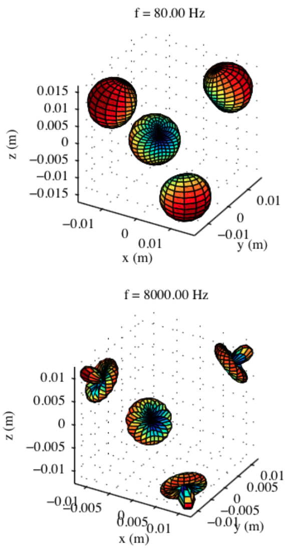

Figure 17 – Geometrical representation of the capsules [Bat09]

In [Bat09] the disturbance of the polar pattern in B-format was highlighted. This fact results from two physical reasons: first of all, for evident practical reasons the capsules are spaced apart, which leads to non-coincidence and *spatial aliasing*. For high frequencies, where the half of wavelength becomes in the same dimension as the distance between the capsules, an undesired cancellation of signals in the W-channel and enhancement in other B-format channels is measured.
Another reason is the distortion of its directivity pattern since a decay of sensitivity of each capsule occurs when the capsule size gets in the same dimension as the wavelength and the diaphragm is hit sideways from the impinging wave. This case is shown in figure 17 (bottom). Following figures 18 show the directivity patterns of W- and Z-component in B-format. At 8kHz it seems that the components do not keep the ideal polar patterns at all.

4.4 Validity of Soundfield microphone

As stated in the above section, the polar patterns in B-format are disturbed from a certain frequency. By observing the LF-values issued from the experiment, we could notice how

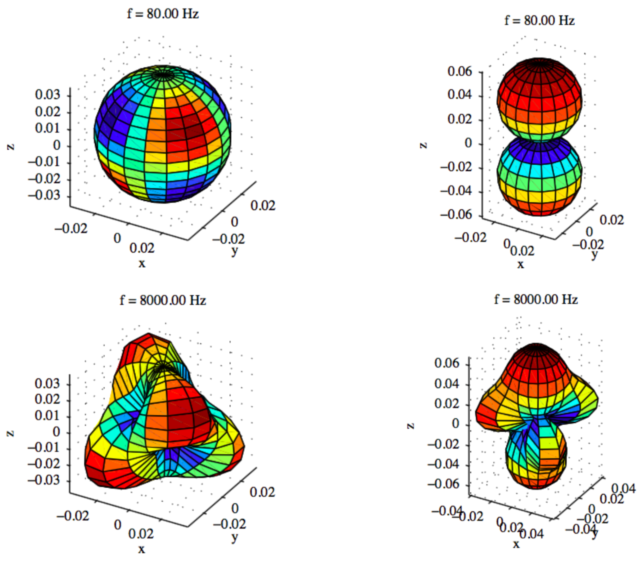

(a) W-component in B-Format (b) Z-component in B-Format

Figure 18 – B-format representation at 80 Hz and 8 kHz [Bat09]

strong the distortion of the polar pattern in B-format affects the LF.
Figure 20 highlights these disturbances, for instance the LF-value at 4kHz octave-band represents an unrealisable value.

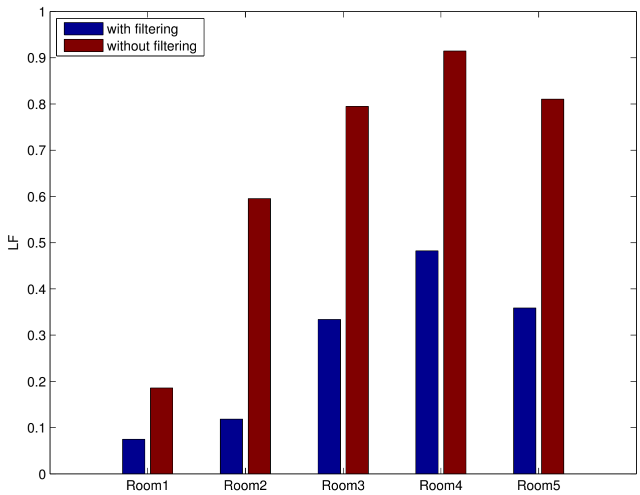

Figure 19 – Influence of a low-pass filter (3.2kHz) with the SPS200 (Appendix F)

The spatial aliasing becomes already perturbing as $\frac{\lambda}{4}$ gets smaller than the distance between two capsules of SPS200 ($d \approx 5.7cm$) and even more when $\frac{\lambda}{2}$ goes smaller than d. It can also be noticed that the LF-values go quite bad from 3kHz ($\lambda \approx 11.4$cm). For this reason it might be reasonable to filter out high frequencies. The influence of a 3.2kHz

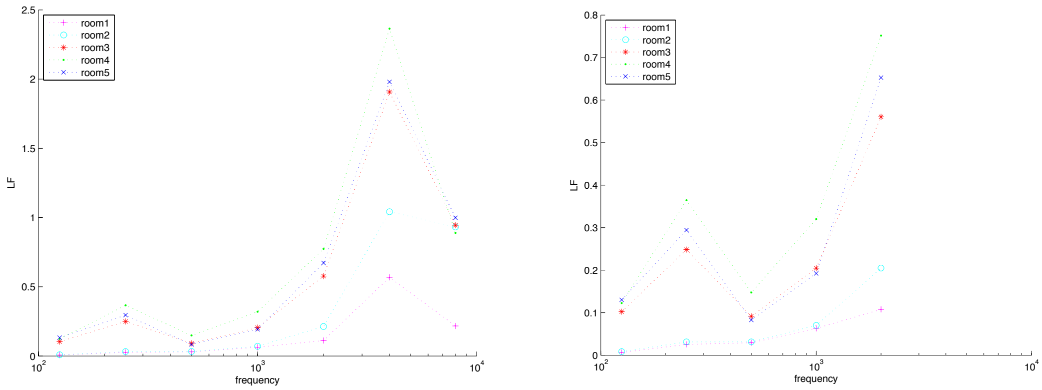

(a) without filter (b) with filter

Figure 20 – LF values with soundfield microphone

Butterworth-low-pass filter of 10th order is shown in figure 19 and 20. Thus, the spatial aliasing seems to affect the values of LF for high frequencies and therefore also the broadband LF-value.

In [Bat09], a way to design a filter to reduce the effect of spatial aliasing was discussed, the W channel as well as the X, Y and Z channels were equalized. However, the spectrum of amplitude is strongly dependent on the incidence of the wave. For these reasons, the use of a tetrahedron microphone without any correction and even with a simple spectral correction might not be convenient for the determination of LF.

5 Spatial fluctuations of LF

This chapter deals with spatial fluctuations of lateral energy fraction, i.e. a significant variation of measured LF-values with small displacements of measurement positions. It results from the interference phenomenon of wave components in a sound field. For this reason a LF-value measured at one position might be unreliable. In order to guarantee the reliability of the local LF, averaging values measured at multiple measurement positions, is considered. An experiment was undertaken to demonstrate the influence of the position.

5.1 Defining the phenomenon

For a long time, fluctuations of impulse responses and their derived parameters with respect to small displacement of source and microphone have been observed in many studies [dVEMHJB01].
Okano *et al.* measured lateral energy fractions in 555 positions in the Amsterdam Concertgebouw [TOH98] and de Vries *et al.* observed the large fluctuations of the LF, which are not perceived by human ear [dVEMHJB01]. Figure 21 shows LF-fluctuations for the octave bands of 125, 250, 500 and 1000 Hz, an average value and a value for the full bandwidth as a function of microphone offset in Amsterdam Concertgebouw. The fluctuations show an almost-periodicity with offset. Therefore, de Vries *et al.* concluded that the local LF-values do not correspond with a certain ASW, in other words, the local values are useless for the measurement of ASW.

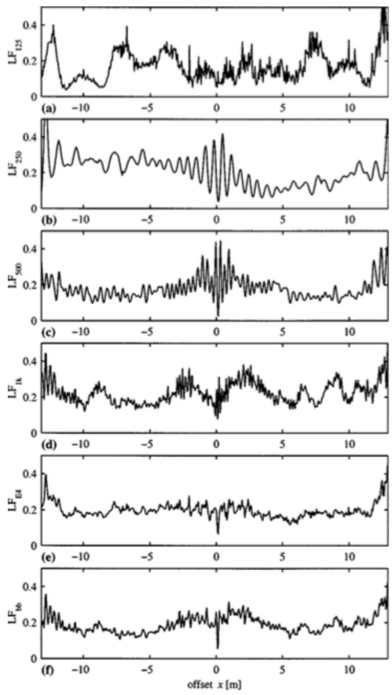

Figure 21 – LF fluctuations

5.2 Multiple measurement positions

The fluctuation problem of local LF-values is improved by averaging values measured at multiple positions as following :

$$\mathrm{LF} = \frac{1}{N}\sum_{i=1}^{N} \mathrm{LF}_i, \tag{16}$$

where N is the number of measurement positions. This idea was suggested in [Fra13] and the author presented that the LF averaged by values measured at two measurement positions with a distance of 14cm correlates with the perceived width of a source. The suggested distance of 14cm, resembling the averaged diameter of human head, has a lower frequency boundary of about 1.2kHz at which the signal is completely decorrelated. Although most of frequencies for LF are under this lower frequency boundary, that is to say, the frequencies related to LF keep a high correlation between two positions with the distance of 14cm, the reasonable result was deducted in his experiment, presenting a high correlation of the LF-value with a perceived source width.

5.3 Comparison of the obtained results

In order to show fluctuations of LF and therefore the necessity for the alternative method consisting of measurement at multiple positions, the measurement was conducted at an off-center $7cm$ from side to side, totally 14cm distance, same as in [Fra13].
The LF-values measured by the two microphones at three measurement positions are given in figure 25. The letter E indicates the center, A 7cm off to the left and B 7cm to the right. The averaged LF of A and B is also shown.
It is observed that the difference of LF in position A and B is quite considerable, for instance the difference is 0.08, (1.6 JND).

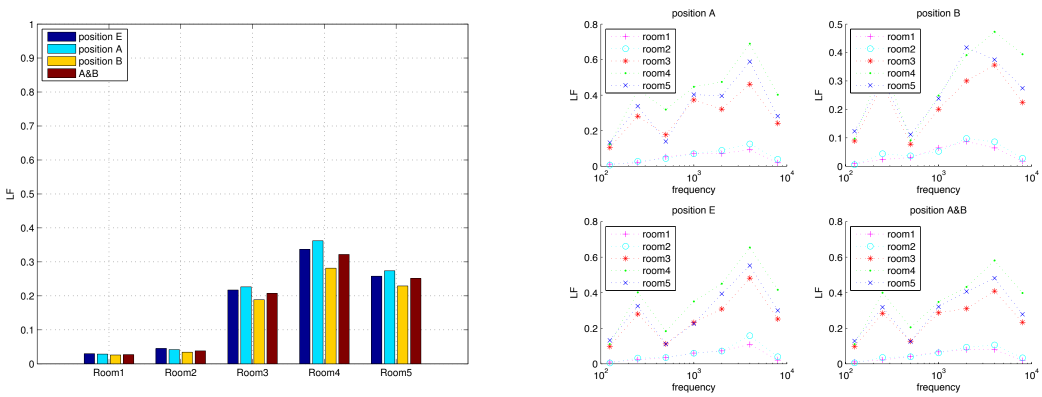

(a) broadband (b) per octave-band

Figure 22 – LF depending on measurement position

6 Psychoacoustical evaluation

To prove how the LF-values in the rooms correspond to the auditive perception of human being, all situations were recorded by a artificial head with variations of measurement positions and delay-time of reflections. Then, a mono audio signal (piano piece) was convolved with the binaural spatial impulse responses derived from the artificial head recordings. 15 people were then asked to *"rate the perceived source width"*.

The test consisted of three parts :
— Evaluation of perceived source width for each room.
— Evaluation of perceived source width between two different positions.
— Evaluation of perceived source width between two different reflection delays.

For every test, the subject had to listen to 10 audio samples randomly sorted as many times he or she wished, to compare and rate them on a scale with a GUI slide. The only given scale indications were simply *narrow* and *wide* on both extremity of the slide (respectively *schmal* and *breit* in german).
The test stops when the subject closes the window. The GUI then returns a value between 1 and 11 for each sample.
Since each subject scaled differently, an average scaling for each test-person and each test was necessary and was realized this way: $x'_i = x_i - \mu_i$ (for each test person), where μ is the average of the values.

6.1 Evaluation of perceived source width for each room

Figure 23 shows the resulting rated data in a box-plot diagram. A high correlation between evaluations and LF-values could be noticed:
At first glance, rooms 1 and 2 have relative lower values of LF compared to rooms 3, 4 and 5, then the determination of the Spearman's rank correlation coefficient gives $\rho = 1$.
Room 4 has the largest LF. A noticeable observation can be made between room 1 and 2: even though the LF-difference between these two rooms stays merely within 1 JND (0.05) (see figure 14), a perceptual difference is obviously distinguished by human ears.
For this reason we might suppose that JND is smaller than 0.05 in the range of very small LF. However, according to [TJC93] the result is opposite, i.e. the JND tends to increase in the range of small LF.
To attempt to explain these observations, we also calculated IACC (which is the other significant parameter for ASW) of room 1 and 2 (see Appendix G). Nevertheless, we observe few differences between the IACC of room 1 and 2. Figure 25(b) shows $1-\text{IACC}_{E3}$ (averaged by 500Hz, 1kHz and 2kHz and time boundaries of 0ms to 80ms).

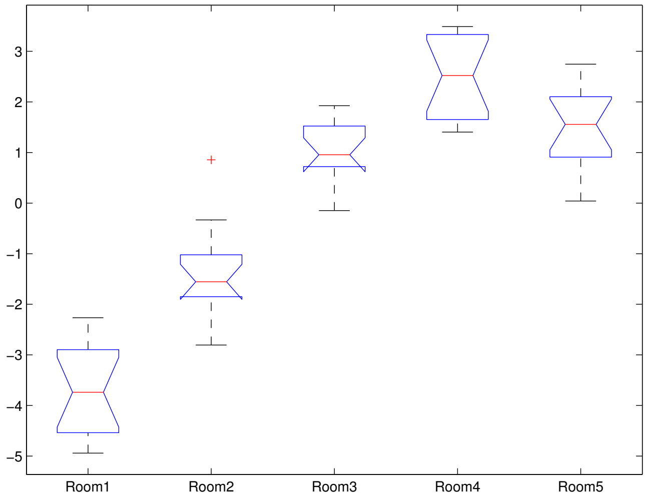

Figure 23 – Evaluation of perceived source width for each room (position E, delays 1)

6.2 Evaluation of perceived source width between two different positions

In figure 24 the statistical results of the varied measurement positions are depicted. In total 9 variations and a test-sample (two times Room 5 position A) were evaluated. Even if the LF-values between the positions in the room 3, 4 and 5 present obvious differences (see figure 22(a)), it seems that the participants perceive few differences. Furthermore, in natural hearing situation, moving the head may improve the correlation between ASW and LF.
In conclusion the fluctuation of LF-values with a small displacement variation is not perceived, even though the calculation yields a large difference of LF.

6.3 Evaluation of perceived source between two different reflection delays

The statistical results of the varied reflection delays are shown in the figure 26. A remarkable fact is that the participants perceived a significant difference of ASW in the same room with different delay-times of the reflections, even though the LF-values of both situations stay within 1 JND (see figure 25(a)). At first sight without any further investigations, it seems that the later the reflecting energy, the narrower the source is perceived. $IACC_{E3}$ for delay 1 and 2 were also calculated to distinguish the difference. However, only small differences were observed between the delay 1 and 2 (see figure 25(b)).

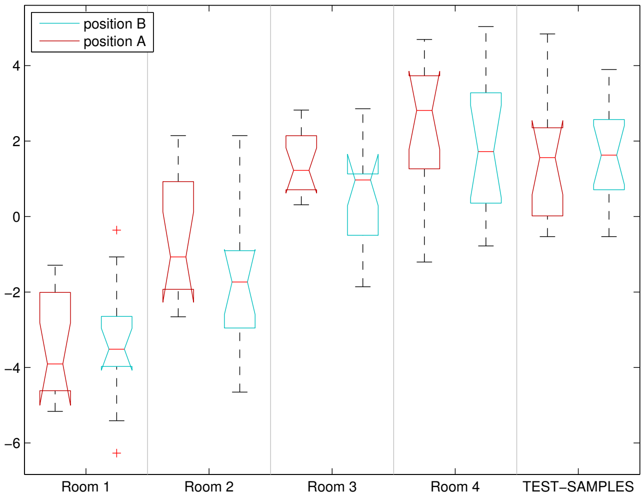

Figure 24 – Evaluation of perceived source width between two different positions (A and B)

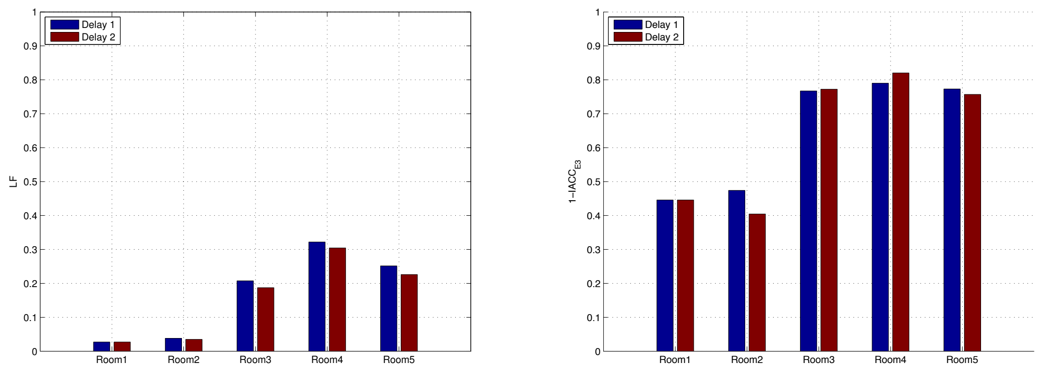

(a) LF

(b) $1-\mathrm{IACC}_{E3}$

Figure 25 – LF and $1-\mathrm{IACC}_{E3}$ for delay 1 and delay 2

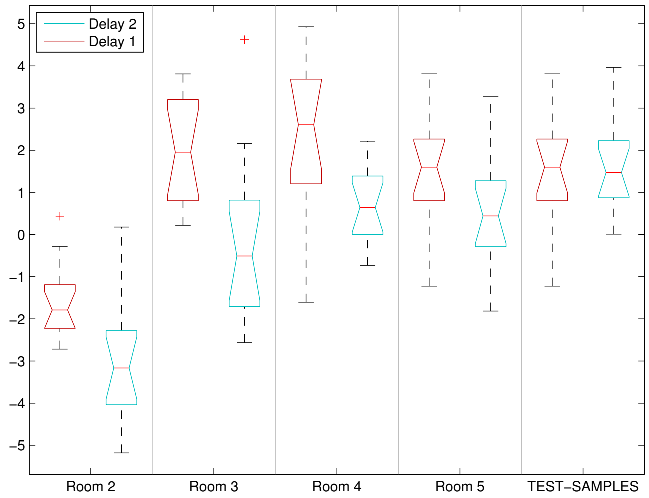

Figure 26 – Evaluation of perceived source width between two different reflection delays

7 Conclusion

In this work, various sources of imprecision in the determination of LF have been investigated. The influence of *spacing* or *orientation* are negligible in some degree. On the contrary, *pick-up pattern*, *gain* and *spectrum* may have a huge effect on the measurement of LF. The spectrum as well as the gain between two different microphones should be calibrated with a minimum phase filter to obtain precise LF.
It has been demonstrated that the use of a tetrahedral microphone array might not be the best option due to strong disturbances of the pickup-pattern and spectrum in B-format. Although this effect could be partly avoided by using an averaged spectral correction filter, however, this problem cannot be totally solved since the spectrum and sensitivity depend strongly on the incidence of the sound.
The spatial fluctuations of LF also play a significant role in determining LF and it has been shown that LF in a measurement position with a small offset yield a considerable difference; for this reason it has been proposed to conduct two measurements with a distance of 14cm and average them.
At last, the correspondence between ASW and LF has been highlighted by conducting a series of psychoacoustic tests. A discordance between ASW and LF has been observed in rooms with lower LF; an obvious perceptual difference between room 1 and 2 appeared, even though the LF-values are highly similar to each other. Another parameter for ASW, *IACC*, could not explain the discordance as well. In addition, it has been observed that the participants do not perceive a difference of ASW between two measurement positions with a small offset, even if LF-values at the two positions are quite different. Furthermore, it seems that the temporal distribution of sound energy within the 80ms time boundary may affect the perceived ASW: the later the reflections, the narrower the source was perceived.

List of Figures

List of Tables

References

[Amb] [Online]. Available: http://en.wikipedia.org/wiki/Ambisonics

[Bar71] M. Barron, "The subjective effects of first reflections in concert hall - the need for lateral reflections," *Journal of Sound and Vibration*, vol. 15, no. 4, pp. 475–494, 1971.

[Bat09] J.-M. Batke, "The b-format microphone revised," in *Ambisonics Symposium*, June 2009.

[Beh03] I. W. G. K. Behler, "Der einfluss der mikrophonrichtcharakteristik auf den lateral fraction - parameter," 2003.

[Ber62] L. L. Beranek, *Music, Acoustics, and Architecture*. Wiley, 1962.

[BM81] M. Barron and A. Marshall, "Spatial impression due to early lateral reflections in concert halls: The derivation of a physical meausre," *Journal of Sound and Vibration*, vol. 77, no. 2, pp. 211–232, 1981.

[dVEMHJB01] D. de Vries; Edo M. Hulsebos; Jan Baan, "Spatial fluctuations in measures dor spaciousness," *Journal of the Acoustical Society of America*, vol. 110, no. 2, p. 947, August 2001.

[Fra13] M. Frank, "Phantom sources using mutiple loudspeakers in the horizontal plane," Ph.D. dissertation, Institut für Elektronische Musik und Akustik, 2013.

[ISO09] "Akustik-messung von raumakustischen parametern," ISO, 2009.

[JB86] W. L. J. Blauert, "Auditory spaciousness: Some further psychoacoustic analyses," *Journal of the Acoustical Society of America*, vol. 80, no. 2, pp. 533–541, 1986.

[JB95a] G. S. J.S. Bradley, "The influence of late arriving energy on spatial impression," *Journal of the Acoustical Society of America*, vol. 97, no. 4, pp. 2263–2271, 1995.

[JB95b] ——, "Objective measures of listener envelopment," *Journal of the Acoustical Society of America*, vol. 98, no. 3, pp. 2590–2597, 1995.

[Mar67] A. Marshall, "A note on the importance of room cross-section in concert halls," *Journal of the Acoustical Society of America*, vol. 5, pp. 100–112, 1967.

[Mar68] ——, "Levels of reflection masking in concert halls," *Journal of Sound and Vibration*, vol. 7, pp. 116–118, 1968.

[MCVS13] C. B. G. M. C. Vigeant and A. C. Scherma, "Repeatability of spatial measures using figure-of-eight microphones," *Applied Acoustics*, vol. 74, no. 9, 2013.

[MM88] Z. M. M. Morimoto, "Effects of low frequency components on auditory spaciousness," *Acustica*, vol. 66, pp. 190–196, 1988.

[TH95] T. O. T. Hidaka, L. L. Beranek and, "Interaural cross-correlation, lateral fraction, and low- and high-frequency sound levels as measures of acoustical quality in concert halls," *The Journal of the Acoustical Society of America*, vol. 98, no. 2, pp. 988–1007, 1995.

[TJC93] Y. W. L. T. J. Cox, W. J. Davies, "The sensitivity of listeners to early sound field changes in auditoria," *Acustica*, vol. 79, pp. 27–41, 1993.

[TOH98] L. L. B. T. Okano and T. Hidaka, "Relations among interaural cross-correlation coefficient, lateral fraction, and apparent source width in concert halls," *Journal of the Acoustical Society of America*, vol. 104, pp. 255–265, 1998.

A Appendix 0: Structure of Matlab files

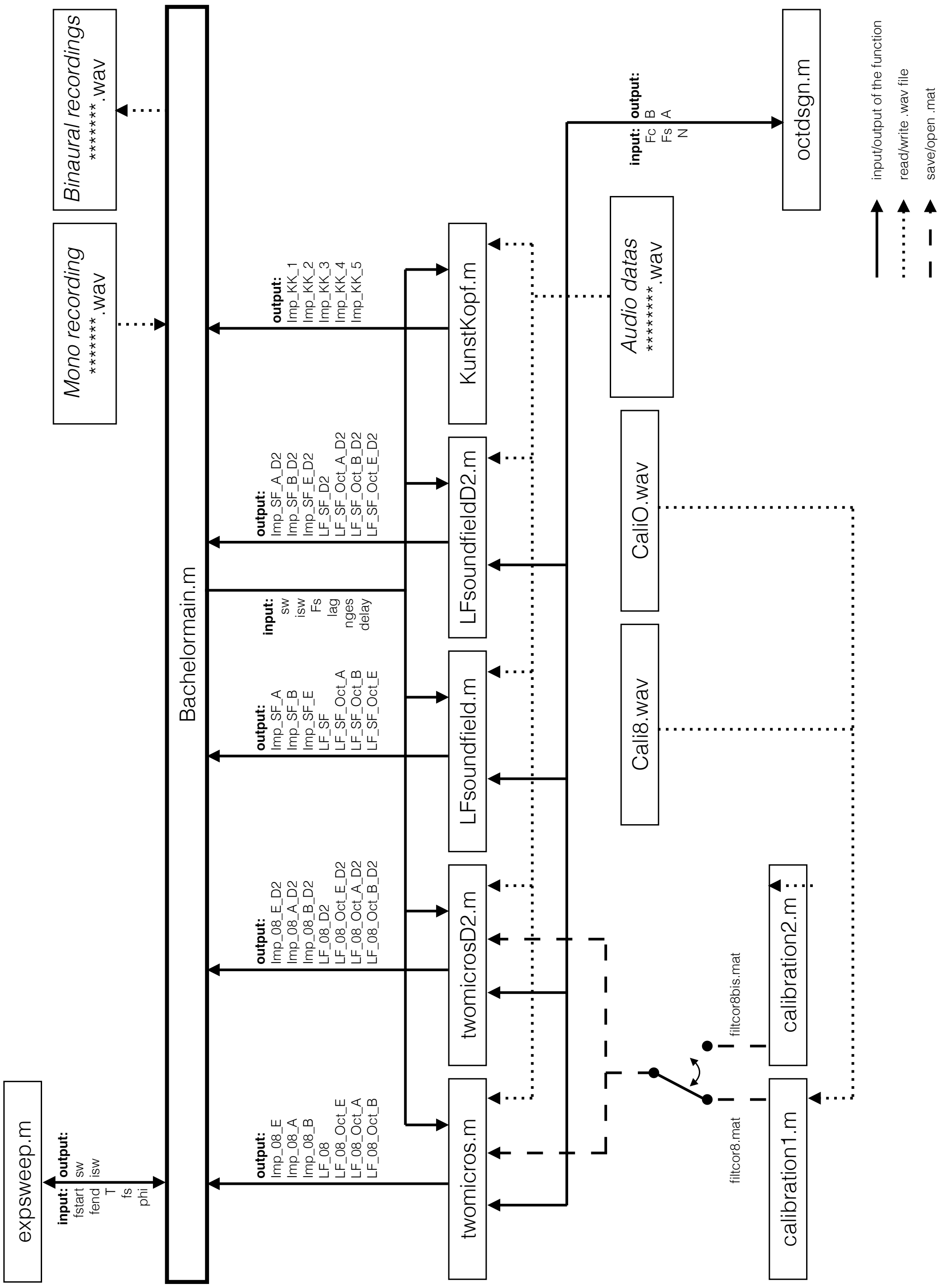

B Appendix 1: *orientation.m*

```
%orientation
clear all
close all
%%
fstart=60;       %begin frequency of sweep
fend=20000;      %end frequency of sweep [hz]
T=3;             %time after sweep (for room response)
Fs=44100;        %sampling frequency
[sw, isw] = expsweep(fstart,fend,T,Fs); %sweep
sw=[zeros(44100,1);sw;zeros(44100,1)];  %sweep
t0 = tukeywin(44100*8,0.002);
t1=t0(length(t0)/2:end,1);
t1=[t1;zeros(44100-1,1)];
sw=sw.*t1; %to avoid clip at the end of the sweep

lag=T*44100;         %define length
nges=length(sw)+length(isw)+lag-1;%number of points in fft (fast conv.)

delay=67404;%67412;  % to get the begin of Imp.-Resp. at 1 (latence)
%%
correctW=1/sqrt(2);
correctY=1;
% READ sweep-resp. from each caps for each room (R1:R5) and pos. (E,A,B)
load('FILTER_Obj_3200.mat');
wb=waitbar(0,'sweep␣responses␣are␣beeing␣read');
wait=0;
pos = ['E'];% 'A' 'B'];
caps= ['L' 'R' 'L' 'R'];
caps2=['F' 'F' 'B' 'B'];
caps3=['U' 'D' 'D' 'U'];
for ii=1:5;
for ns=1:length(pos);  % name variables E,A,B
for nc=1:4;
    eval(['file=''' [caps(nc) caps2(nc)] '_' [pos(ns)] '_' num2str(ii)...
        '.wav'';'])
    eval([[caps(nc) caps2(nc) caps3(nc)] '_' num2str(ii) '_' [pos(ns)]...
        '=audioread(file);'])
    wait=wait+1;
    waitbar(wait/(4*length(pos)*5))
end;
end;
end;
close(wb);

%%%%%%%%%%%%%%%%%%%%%%%%%%%%%%%%
% converting sweep response to B-FORMAT (only W, X and Y)  + LP filter
% (3200Hz)(FILTER_Obj_3200)
wb=waitbar(0,'sweep␣responses␣are␣being␣converted␣to␣B-format');
wait=0;
for ii=1:5;
for ns=1:length(pos);
    %X : fig-8
```

```
eval(['X_' num2str(ii) '_' [pos(ns)] '=(LFU_' num2str(ii) '_' [pos(ns)]...
    '+RFD_' num2str(ii) '_' [pos(ns)] '-LBD_' num2str(ii) '_' [pos(ns)]...
    '-RBU_' num2str(ii) '_' [pos(ns)] ');' ]);
    %filtering high frequencies (over 3000Hz)
    eval(['X_' num2str(ii) '_' [pos(ns)] '=filter(FILTER_Obj_3200,X_'...
        num2str(ii) '_' [pos(ns)] ');'])

    %Y : fig-8
eval(['Y_' num2str(ii) '_' [pos(ns)] '=(LFU_' num2str(ii) '_' [pos(ns)]...
    '-RFD_' num2str(ii) '_' [pos(ns)] '+LBD_' num2str(ii) '_' [pos(ns)]...
    '-RBU_' num2str(ii) '_' [pos(ns)] ');' ]);
    %filtering high frequencies (over 3000Hz)
    eval(['Y_' num2str(ii) '_' [pos(ns)] '=filter(FILTER_Obj_3200,Y_'...
        num2str(ii) '_' [pos(ns)] ');'])

    %W : omni
eval(['W_' num2str(ii) '_' [pos(ns)] '=(LFU_' num2str(ii) '_' [pos(ns)]...
    '+RFD_' num2str(ii) '_' [pos(ns)] '+LBD_' num2str(ii) '_' [pos(ns)]...
    '+RBU_' num2str(ii) '_' [pos(ns)] ');' ]);
    %filtering high frequencies (over 3000Hz)
    eval(['W_' num2str(ii) '_' [pos(ns)] '=filter(FILTER_Obj_3200,W_'...
        num2str(ii) '_' [pos(ns)] ');'])
wait=wait+1;
waitbar(wait/(length(pos)*5));
end
end
close(wb);



%%%%%%%%%%%%%%%%%%%%%%%%%%%%%%%%%
%IMPULS-RESPONSE calculation (80ms) (schnelle Faltung)
for ii=1:5;
for ns=1:length(pos);
    eval(['hX_' num2str(ii) '_' [pos(ns)] '=real(ifft(fft(X_' ...
        num2str(ii) '_' [pos(ns)] ',nges).*fft(isw,nges)));']);
    eval(['hX_' num2str(ii) '_' [pos(ns)] '=correctY*hX_' num2str(ii)...
        '_' [pos(ns)] '(length(isw)+delay:length(isw)+delay+3528);']);
    %deleting first 5ms
    eval(['hX_' num2str(ii) '_' [pos(ns)] '(1:200,1)=0;']);

    eval(['hY_' num2str(ii) '_' [pos(ns)] '=real(ifft(fft(Y_' ...
        num2str(ii) '_' [pos(ns)] ',nges).*fft(isw,nges)));']);
    eval(['hY_' num2str(ii) '_' [pos(ns)] '=correctY*hY_' num2str(ii)...
        '_' [pos(ns)] '(length(isw)+delay:length(isw)+delay+3528);']);
    %deleting first 5ms
    eval(['hY_' num2str(ii) '_' [pos(ns)] '(1:200,1)=0;']);

    eval(['hW_' num2str(ii) '_' [pos(ns)] '=real(ifft(fft(W_' ...
        num2str(ii) '_' [pos(ns)] ',nges).*fft(isw,nges)));']);
    eval(['hW_' num2str(ii) '_' [pos(ns)] '=correctW*hW_' num2str(ii)...
        '_' [pos(ns)] '(length(isw)+delay:length(isw)+delay+3528);']);
end;
end;
```

```
%%%%%%%%%%%%%%%%%%%%%%%%%%%%%%%
% rotation around Z,axis
ANGLE=[0 1 2 3 4 5 10 15 20 30 40 45];
for angle=ANGLE; %degree
anglerad=pi*angle/180;
coefX=sin(anglerad);
coefY=cos(anglerad); % when angle=0 => only Y-axis


%ENERGY & LF in 80ms for both W & Y !
for ii=1:5;
for ns=1:length(pos);
    %rotated Y:
    eval(['hYr_' num2str(ii) '_' [pos(ns)] '(1:3528)=coefX*hX_' ...
        num2str(ii) '_' [pos(ns)] '(1:3528)+coefY*hY_' num2str(ii) '_' ...
        [pos(ns)] '(1:3528);']);
    %3528 samples in 80ms @ 44100Hz
    eval(['eYr_' num2str(ii) '_' [pos(ns)] '=sum(hYr_' num2str(ii)...
        '_' [pos(ns)] '.^2);'])
    eval(['eW_' num2str(ii) '_' [pos(ns)] '=sum(hW_' num2str(ii) '_' ...
        [pos(ns)] '(1:3528).^2);'])

    eval(['ELEF_' num2str(ii) '_' [pos(ns)] '_' num2str(angle) '=eYr_' ...
        num2str(ii) '_' [pos(ns)] '/eW_' num2str(ii) '_' [pos(ns)] ';'])
end
end
end;

%result matrix (col: #room ; line: degree)
for ii=1:5;
for i=1:length(ANGLE)
eval(['ELEF(i,ii)=ELEF_' num2str(ii) '_E_' num2str(ANGLE(i)) ';']);
end;
end;

figure ('name','Orientation')
bar(ELEF')
ylabel('LF')
legend(strcat(num2str(ANGLE'),'°'),'Location','NorthWest');
set(gca,'xticklabel',{'Room1','Room2','Room3','Room4','Room5'});
```

C Appendix 2: *calibrationI.m*

```
%% ---------- SWEEP --& other values-------------
fstart=60;      %begin frequency of sweep
fend=20000;     %end frequency of sweep [hz]
T=3;            %time after sweep (for room response)
Fs=44100;       %sampling frequency
[sw, isw] = expsweep(fstart,fend,T,Fs);
sw=[zeros(44100,1);sw;zeros(44100,1)];  %sweep

lag=3*44100;        %define length
nges=length(sw)+length(isw)+lag-1;  %num of pts in fft (precision for IR)
nv=220; %number of samples before first reflection
delay=66990; %to adjust Imp.resp. on 1
%% %%%%%%%%%%%%%%%%%%%%%%%%%%%%%%%%%
% getting calibration sweep response (close to LS to delay 1st reflections)
[y8]=audioread('Cali8.wav');
[y0]=audioread('Cali0.wav');

    %%%%%%%%%%%%%%%%%%%%%%%%%%%%%%%%
h8=real(ifft(fft(y8,nges).*fft(isw,nges)));
    h8=h8(length(isw)+delay:length(isw)+delay+nv-1);
    h8=[h8;zeros(44100-length(h8),1)];%Impuls Response (+zero padding!)

h0=real(ifft(fft(y0,nges).*fft(isw,nges)));
    h0=h0(length(isw)+delay:length(isw)+delay+nv-1);
    h0=[h0;zeros(44100-length(h0),1)];%Impuls Response (+ zero padding!)


    %filtering
    %Division in octave band
[B_31,A_31] = octdsgn(31,Fs,3);%coeffs for 75Hz oct-band
[B_63,A_63] = octdsgn(63,Fs,3);%coeffs for 75Hz oct-band
[B_125,A_125] = octdsgn(125,Fs,3);%coeffs for 125Hz oct-band
[B_250,A_250] = octdsgn(250,Fs,3);%coeffs for 250Hz oct-band
[B_500,A_500] = octdsgn(500,Fs,3);%coeffs for 500Hz oct-band
[B_1000,A_1000] = octdsgn(1000,Fs,3);%coeffs for 1kHz oct-band
[B_2000,A_2000] = octdsgn(2000,Fs,3);%coeffs for 2kHz oct-band
[B_4000,A_4000] = octdsgn(4000,Fs,3);%coeffs for 4kHz oct-band
[B_8000,A_8000] = octdsgn(8000,Fs,3);%coeffs for 4kHz oct-band

% determination of correction factor for each octave band
for oct=[31 63 125 250 500 1000 2000 4000 8000]
    %Imp-Response
    eval(['h8_' num2str(oct) '=filter(B_' num2str(oct) ',A_' ...
        num2str(oct) ',h8);'])
    eval(['h0_' num2str(oct) '=filter(B_' num2str(oct) ',A_' ...
        num2str(oct) ',h0);'])
    %energy
    eval(['e8_' num2str(oct) '=sum(h8_' num2str(oct) '.^2);']);
    eval(['e0_' num2str(oct) '=sum(h0_' num2str(oct) '.^2);']);
    %correction coefficient for each oct.-band (linear gain)
    eval(['coeff_' num2str(oct) '=sqrt(e0_' num2str(oct) '/e8_' ...
        num2str(oct) ')'])
```

```
end;

f0=abs(fft(h0));
f8=abs(fft(h8));
coeff_22050=f0(22050)/f8(22050);
coeff_1=f0(1)/f8(1);

%creating a correction spectrum for fig-8
%oct-bands
xcorrect=[0 31 63 125 250 500 1000 2000 4000 8000 Fs/2];
%correct-fact. for each oct-band
ycorrect=[coeff_1 coeff_31 coeff_63 coeff_125 coeff_250 coeff_500 ...
    coeff_1000 coeff_2000 coeff_4000 coeff_8000 coeff_22050];
xx=[0:1:44100/2];
%interpolation of spectrum from oct-band correction filter
correctf=interp1(xcorrect,ycorrect,xx,'pchip'); % piecewise cubic interp.
correctf=[correctf,fliplr(correctf(2:end-1))];


%creating a minimalphase filter with the help of cepstral domain
w = [1;2*ones(Fs/2-1,1);ones(1-rem(Fs,2),1);zeros(Fs/2-1,1)];
y = real(ifft(log(correctf))); %cepstrum
ym = real(ifft(exp(fft(w.*y'))));% time domain & minimum-phase

save('filtcor8.mat','ym')

%spectrum of designed minimal-phase filter
fym=abs(fft(ym));

figure('name','design␣of␣minimal-phase␣filter␣for␣fig-8␣2')
subplot(2,1,1)
hold on
plot(xcorrect(1:end-1),20*log10(ycorrect(1:end-1)),'.','MArkerSize',10);
plot(xx,20*log10(correctf(1:Fs/2+1)),'r-','Linewidth',0.5)
hold off
set(gca,'XScale','log')
legend('correction␣factor␣for␣each␣octave',...
    'linear␣interpolation␣of␣the␣correction␣factors')
title('desired␣spectrum␣for␣the␣correction␣filter')
subplot(2,1,2)
plot(20*log10(fym))
set(gca,'XScale','log')
title('spectrum␣of␣the␣correcting␣filter␣(minimum␣phase)')
```

D Appendix 3: *calibrationII.m*

```
%% ---------- SWEEP --& other values-------------
fstart=60;       %begin frequency of sweep
fend=20000;      %end frequency of sweep [hz]
T=3;             %time after sweep (for room response)
Fs=44100;        %sampling frequency
[sw, isw] = expsweep(fstart,fend,T,Fs);
sw=[zeros(44100,1);sw;zeros(44100,1)];  %sweep

lag=3*44100;         %define length
nges=length(sw)+length(isw)+lag-1;  %num of pts in fft (precision for IR)
nv=220; %number of samples before first reflection)
delay=66990; %to adjust Imp.resp. on 1
%% %%%%%%%%%%%%%%%%%%%%%%%%%%%%%%%%%
% getting calibration sweep response (close to LS to delay 1st reflections)
[y8]=audioread('Cali8.wav');
[y0]=audioread('Cali0.wav');

    %%%%%%%%%%%%%%%%%%%%%%%%%%%%%%%%
h8=real(ifft(fft(y8,nges).*fft(isw,nges)));
    h8=h8(length(isw)+delay:length(isw)+delay+nv-1);
    h8=[h8;zeros(44100-length(h8),1)];%Impuls Response (+zero padding!)

h0=real(ifft(fft(y0,nges).*fft(isw,nges)));
    h0=h0(length(isw)+delay:length(isw)+delay+nv-1);
    h0=[h0;zeros(44100-length(h0),1)];%Impuls Response (+zero padding!)


correctf=abs(fft(h0))./abs(fft(h8)); %spectral division

%creating a MINIMAL-PHASE FILTER with the help of cepstral domain
w = [1;2*ones(Fs/2-1,1);ones(1-rem(Fs,2),1);zeros(Fs/2-1,1)]; %Hilbert Tr.
y = real(ifft(log(correctf))); %CEPSTRUM
ym = real(ifft(exp(fft(w.*y))));% -> minimum-phase -> time domain

save('filtcor8bis.mat','ym')

%spectrum of designed minimal-phase filter
fym=abs(fft(ym)); %spectrum of min.-ph.filt.
xx=[0:1:44100/2];

figure('name','design␣of␣minimal-phase␣filter␣for␣fig-8␣␣')
subplot(2,1,1)
plot(xx,20*log10(correctf(1:Fs/2+1)),'r-','Linewidth',0.5)
%axis([0 Fs 0 2.5]);
set(gca,'XScale','log')
title('spectral␣division␣between␣omni␣and␣fig.-8')
subplot(2,1,2)
plot(20*log10(fym))
set(gca,'XScale','log')
title('spectrum␣of␣the␣correcting␣filter␣(minimum␣phase)')
```

E Appendix 4: *twomicros.m*

```
function [ imp_08_E imp_08_A imp_08_B LF_08 LF_08_Oct_E LF_08_Oct_A ...
    LF_08_Oct_B] = twomicros(sw,isw,Fs, lag, nges, delay)
%2micros: reads sweep-responses, do deconvolution, returns:
%   -imp_08_°                    (°= 3 positions E,A,B)
%                                column: #room (alternate 8/omni)
%                                line:   samples
%   -LF_08                       column: #room
%                                line: position (A,B,E)
%   -LF_08_°_oct                 (°= 3 positions A,B,E)
%                                column: #room
%                                line:   oct-band number (125 to 2kHz)
%%%%%%%%%%%%%%%%%%%%%%%%%%%%%%%%%%%%%%%%%%%%%%%%%%%%%%%%%%%%%%%%%%%

% correction coeffs per oct.band (125 to 2kHz)
c_o=[1.0061 0.7396 0.8057 0.8474 0.9755];
% LOAD FILTER (LP 3200Hz)
load('FILTER_Obj_3200.mat');
% LOAD Imp. resp. of CORRECT.-FILTER for fig-8 (ym)
load('filtcor8bis.mat');

%read sweep-responses - rooms (R1:R5) - positions E,A,B
pos = ['E' 'A' 'B'];
for ns=1:length(pos);
    for ii=1:5;
eval(['[y8' num2str(ii) '_' [pos(ns)] ']=audioread(''ACHTER_' [pos(ns)] ...
    '_' num2str(ii) '.wav'');'])
eval(['[y0' num2str(ii) '_' [pos(ns)] ']=audioread(''OMNI_' [pos(ns)] ...
    '_' num2str(ii) '.wav'');'])
% % FILTERING HIGH FREQUENCIES (above 3200Hz)   -  OPTIONNAL !!!
% eval(['[y8' num2str(ii) '_' [pos(ns)] ']=filter(FILTER_Obj_3200,y8' ...
%     num2str(ii) '_' [pos(ns)] ');'])
% eval(['[y0' num2str(ii) '_' [pos(ns)] ']=filter(FILTER_Obj_3200,y0' ...
%     num2str(ii) '_' [pos(ns)] ');'])
    end;
end;


%Impuls-responses calculation
for ns=1:length(pos);
for ii=1:5;
    eval(['h8' num2str(ii) '_' [pos(ns)] '=real(ifft(fft(y8' num2str(ii)...
        '_' [pos(ns)] ',nges).*fft(isw,nges)));']);
    eval(['h8' num2str(ii) '_' [pos(ns)] '=h8' num2str(ii) '_' [pos(ns)]...
        '(length(isw)+delay:length(isw)+delay+3527);']); %Impuls Response
    %deleting first 5ms (ISO 3382)
    eval(['h8' num2str(ii) '_' [pos(ns)] '(1:200,1)=0;']);
    % convolution with imp.-resp. of correcting filter (ym)
nges2=3528+length(ym)-1; %nbr of points in fft for fast conv.
    eval(['h8C' num2str(ii) '_' [pos(ns)] '=real(ifft(fft(h8' ...
        num2str(ii) '_' [pos(ns)] ',nges2).*fft(ym,nges2)));']);
    eval(['h8C' num2str(ii) '_' [pos(ns)] '=h8C' num2str(ii) '_' ...
        [pos(ns)] '(1:end-length(ym)+1);']);
```

```
    eval(['h0' num2str(ii) '_' [pos(ns)] '=real(ifft(fft(y0' num2str(ii)...
        '_' [pos(ns)] ',nges).*fft(isw,nges)));']);
    eval(['h0' num2str(ii) '_' [pos(ns)] '=h0' num2str(ii) '_' [pos(ns)]...
        '(length(isw)+delay:length(isw)+delay+3527);']); %Impuls Response
end;
end;

figure('name','calibration comparison')
subplot(2,1,1)
hold on
plot(h83_E)
plot(h8C3_E,'r')
legend('before correction','after correction');
hold off
subplot(2,1,2)
hold on
plot(abs(fft(h83_E)))
plot(abs(fft(h8C3_E)),'r')
legend('before correction','after correction');
hold off

% 3 result matrix (pos E, A then B) - 2*5 columns: #room (8 then 0)
% line:samples
for ii=1:5;
    for ns=1:length(pos);
eval(['imp_08_' [pos(ns)] '(:,2*ii-1)=h8C' num2str(ii) '_' [pos(ns)] ';']);
eval(['imp_08_' [pos(ns)] '(:,2*ii)=h0' num2str(ii) '_' [pos(ns)] ';']);
    end;
end;

%energy calculation (80ms)
for ns=1:length(pos);
for ii=1:5; %room 1 to 5
    %LF whole frequence-band
    eval(['e8' num2str(ii) '_' [pos(ns)] '=sum(h8' num2str(ii) '_' ...
        [pos(ns)] '.^2);']);
    eval(['e0' num2str(ii) '_' [pos(ns)] '=sum(h0' num2str(ii) '_' ...
        [pos(ns)] '.^2);']);
    %LFs in result matrix (column: num of room (R1 to R5); line:(E,A,B))
    eval(['LF_08(ns,' num2str(ii) ')=[e8' num2str(ii) '_' [pos(ns)] ...
        '/e0' num2str(ii) '_' [pos(ns)] '];'])
end;
end;


%Division on octave band
oct=[125 250 500 1000 2000]; %usefull for following for-loops
[B1,A1] = octdsgn(125,Fs,3);%coeffs for 125Hz oct-band
[B2,A2] = octdsgn(250,Fs,3);%coeffs for 250Hz oct-band
[B3,A3] = octdsgn(500,Fs,3);%coeffs for 500Hz oct-band
[B4,A4] = octdsgn(1000,Fs,3);%coeffs for 1kHz oct-band
[B5,A5] = octdsgn(2000,Fs,3);%coeffs for 2kHz oct-band
```

```
%%%%%%%%%%%%%%%%%%%%%

for ns=1:length(pos);
    for ii=1:5;  % 5 rooms (R1 to R5)
        for o=1:length(oct);
%filtering signal for each oct-band
eval(['H8' num2str(ii) '_' [pos(ns)] '_' num2str(oct(o)) '=c_o(' ...
    num2str(o) ')*filter(B' num2str(o) ',A' num2str(o) ',h8' num2str(ii)...
    '_' [pos(ns)] ');']);  %filtering signals
eval(['H0' num2str(ii) '_' [pos(ns)] '_' num2str(oct(o)) '=filter(B' ...
    num2str(o) ',A' num2str(o) ',h0' num2str(ii) '_' [pos(ns)] ');']);

%"squaring" and sum (energy)
eval(['e8' num2str(ii) '_' [pos(ns)] '_' num2str(oct(o)) '=sum(H8' ...
    num2str(ii) '_' [pos(ns)] '_' num2str(oct(o)) '.^2);']);
eval(['e0' num2str(ii) '_' [pos(ns)] '_' num2str(oct(o)) '=sum(H0' ...
    num2str(ii) '_' [pos(ns)] '_' num2str(oct(o)) '.^2);']);

%calculate LFs (energy fig8/energy omni) for every octave-band
eval(['LF' num2str(ii) '_' [pos(ns)] '_' num2str(oct(o)) '=e8' ...
    num2str(ii) '_' [pos(ns)] '_' num2str(oct(o)) '/e0' num2str(ii) ...
    '_' [pos(ns)] '_' num2str(oct(o)) ';']);
        end;
    end;
end;



%saving LFs in 3 result-matrix E,A and B (column: num of Room (R1 to R5)
%line:Oct-band)
for ii=1:5;
    for ns=1:length(pos);
        for o=1:length(oct);
eval(['LF_08_Oct_' [pos(ns)] '(' num2str(o) ',' num2str(ii) ')=LF' ...
    num2str(ii) '_' [pos(ns)] '_' num2str(oct(o)) ';']);
        end;
    end;
end;
%%%%%%%%%%%%%%%%%%%%%

end
```

F Appendix 5: *LFsoundfield.m*

```
function [ imp_SF_A imp_SF_B imp_SF_E LF_SF LF_SF_A_Oct LF_SF_B_Oct...
    LF_SF_E_Oct ] = LFsoundfield(sw,isw,Fs, lag, nges, delay)
%2micros: reads sweep-responses, do deconvolution, returns:
%   -imp_SF_°                       (°= 3 positions A,B,E)
%                                   column: #room (alternate Y/W)
%                                   row:   samples
%   -LF_SF                          column: #room
%                                   row: position (A,B,E)
%   -LF_SF_°_oct                    (°= 3 positions A,B,E)
%                                   column: #room
%                                   row:   oct-band (125 to 2kHz)
%%%%%%%%%%%%%%%%%%%%%%%%%%%%%%%%%%%%%%%%%%%%%%%%%%%%%%%%%%%%%%%%%%
%correction gain for Y and W channels
correctW=1/sqrt(2);
correctY=1;
% READ sweep-resp. from each caps for each room (R1:R5) and pos. (E,A,B)
load('FILTER_Obj_3200.mat');
wb=waitbar(0,'sweep␣responses␣are␣beeing␣read');
wait=0;
pos = ['E' 'A' 'B'];
caps= ['L' 'R' 'L' 'R'];
caps2=['F' 'F' 'B' 'B'];
caps3=['U' 'D' 'D' 'U'];
for ii=1:5;
for ns=1:length(pos);  % name variables E,A,B
for nc=1:4;
    eval(['file=''' [caps(nc) caps2(nc)] '_' [pos(ns)] '_' num2str(ii)...
        '.wav'';'])
    eval([[caps(nc) caps2(nc) caps3(nc)] '_' num2str(ii) '_' [pos(ns)]...
        '=audioread(file);'])
    wait=wait+1;
    waitbar(wait/(4*length(pos)*5))
end;
end;
end;
close(wb);

%%%%%%%%%%%%%%%%%%%%%%%%%%%%%%%
% converting sweep response to B-FORMAT (only W and Y) & LP filter
% (3200Hz) (FILTER_Obj_3200)
wb=waitbar(0,'sweep␣responses␣are␣being␣converted␣to␣B-format');
wait=0;
for ii=1:5;
for ns=1:length(pos);
    %Y : fig-8
eval(['Y_' num2str(ii) '_' [pos(ns)] '=(LFU_' num2str(ii) '_' [pos(ns)]...
    '-RFD_' num2str(ii) '_' [pos(ns)] '+LBD_' num2str(ii) '_' [pos(ns)] '-RBU_'
    %filtering high frequencies (over 3000Hz)
   eval(['Y_' num2str(ii) '_' [pos(ns)] '=filter(FILTER_Obj_3200,Y_' ...
       num2str(ii) '_' [pos(ns)] ');'])
    %W : omni
eval(['W_' num2str(ii) '_' [pos(ns)] '=(LFU_' num2str(ii) '_' [pos(ns)]...
```

```
    '+RFD_' num2str(ii) '_' [pos(ns)] '+LBD_' num2str(ii) '_' [pos(ns)]...
    '+RBU_' num2str(ii) '_' [pos(ns)] ');' ]);
    %filtering high frequencies (over 3000Hz)
   eval(['W_' num2str(ii) '_' [pos(ns)] '=filter(FILTER_Obj_3200,W_'...
       num2str(ii) '_' [pos(ns)] ');'])
wait=wait+1;
waitbar(wait/(length(pos)*5));
end
end
close(wb);



%%%%%%%%%%%%%%%%%%%%%%%%%%%%%%%%%
%IMPULS-RESPONSE calculation (80ms) (schnelle Faltung)
for ii=1:5;
for ns=1:length(pos);
    eval(['hY_' num2str(ii) '_' [pos(ns)] '=real(ifft(fft(Y_'...
        num2str(ii) '_' [pos(ns)] ',nges).*fft(isw,nges)));']);
    eval(['hY_' num2str(ii) '_' [pos(ns)] '=correctY*hY_' num2str(ii)...
        '_' [pos(ns)] '(length(isw)+delay:length(isw)+delay+3528);']);
    %deleting first 5ms
    eval(['hY_' num2str(ii) '_' [pos(ns)] '(1:200,1)=0;']);

    eval(['hW_' num2str(ii) '_' [pos(ns)] '=real(ifft(fft(W_' ...
        num2str(ii) '_' [pos(ns)] ',nges).*fft(isw,nges)));']);
    eval(['hW_' num2str(ii) '_' [pos(ns)] '=correctW*hW_' num2str(ii)...
        '_' [pos(ns)] '(length(isw)+delay:length(isw)+delay+3528);']);
end;
end;

%%%%%%%%%%%%%%%%%%%%%%%%%%%%%%%%%
% RESULT matrix (Imp-Resp) one matrix per position (A,B,E)
            %column:    numb. of room (R1 to R5) (alternated Y/W)
            %row:      samples
for ii=1:5;
for ns=1:length(pos);
eval(['imp_SF_' [pos(ns)] '(:,' num2str(2*ii-1) ')=hY_' num2str(ii) ...
    '_' [pos(ns)] ';'])
eval(['imp_SF_' [pos(ns)] '(:,' num2str(2*ii) ')=hW_' num2str(ii) ...
    '_' [pos(ns)] ';'])
end;
end;


%%%%%%%%%%%%%%%%%%%%%%%%%%%%%%%%
%ENERGY & LF in 80ms for both W & Y !
for ii=1:5;
for ns=1:length(pos);
    %3528 samples in 80ms @ 44100Hz
    eval(['eY_' num2str(ii) '_' [pos(ns)] '=sum(hY_' num2str(ii) '_' ...
        [pos(ns)] '(1:3528).^2);'])
    eval(['eW_' num2str(ii) '_' [pos(ns)] '=sum(hW_' num2str(ii) '_' ...
        [pos(ns)] '(1:3528).^2);'])
```

```
    eval(['ELEF_' num2str(ii) '_' [pos(ns)] '=eY_' num2str(ii) '_' ...
        [pos(ns)] '/eW_' num2str(ii) '_' [pos(ns)] ';'])
end
end

% RESULT Matrix LF (whole freq. band)
            %column:    num of room (R1 to R5)
            %row:      position (A,B,E)
for ii=1:5;
for ns=1:length(pos);
eval(['LF_SF(' num2str(ns) ',' num2str(ii) ')=ELEF_' num2str(ii)  '_' ...
    [pos(ns)] ';'])
end;
end;

%%%%%%%%%%%%%%%%%%%%%%%%%%%%%%%%%%%%%%%%%%%%%%%%%%%%%%%%%%%%%%%%%%%%%%%%%%%
%%%%%%%%%%%%%%%%%%%%%%%%%%%%%%%
%Division on octave band
[B_125,A_125] = octdsgn(125,Fs,3);%coeffs for 125Hz oct-band
[B_250,A_250] = octdsgn(250,Fs,3);%coeffs for 250Hz oct-band
[B_500,A_500] = octdsgn(500,Fs,3);%coeffs for 500Hz oct-band
[B_1000,A_1000] = octdsgn(1000,Fs,3);%coeffs for 1kHz oct-band
[B_2000,A_2000] = octdsgn(2000,Fs,3);%coeffs for 2kHz oct-band
%      [B_4000,A_4000] = octdsgn(4000,Fs,3);%coeffs for 1kHz oct-band
%      [B_8000,A_8000] = octdsgn(8000,Fs,3);%coeffs for 2kHz oct-band


for ii=1:5;
for ns=1:length(pos);
for oct=[125 250 500 1000 2000 ]%4000 8000]
    %Imp-Response post filtering
    eval(['hY_' num2str(ii) '_' [pos(ns)] '_' num2str(oct) '=filter(B_'...
        num2str(oct) ',A_' num2str(oct) ',hY_' num2str(ii) '_' [pos(ns)]...
        ');'])
    eval(['hW_' num2str(ii) '_' [pos(ns)] '_' num2str(oct) '=filter(B_'...
        num2str(oct) ',A_' num2str(oct) ',hW_' num2str(ii) '_' [pos(ns)]...
        ');'])
    %energy
    eval(['eY_' num2str(ii) '_' [pos(ns)] '_' num2str(oct) '=sum(hY_'...
        num2str(ii) '_' [pos(ns)] '_' num2str(oct) '.^2);']);
    eval(['eW_' num2str(ii) '_' [pos(ns)] '_' num2str(oct) '=sum(hW_'...
        num2str(ii) '_' [pos(ns)] '_' num2str(oct) '.^2);']);
    %ELEF
    eval(['ELEF_' num2str(ii) '_' [pos(ns)] '_' num2str(oct) '=eY_'...
        num2str(ii) '_' [pos(ns)] '_' num2str(oct) '/eW_' num2str(ii)...
        '_' [pos(ns)] '_' num2str(oct) ';' ])
end;
end;
end;

% Result matrix   |  1 Matrix per position (A,B,E)
%                 |  column: room number (R1 to R5)
%                 |  line: oct.-band (125 to 2kHz)
```

```
for ii=1:5;
for ns=1:length(pos);
    eval(['LF_SF_' [pos(ns)] '_Oct(1,' num2str(ii) ')=ELEF_' num2str(ii)...
        '_' [pos(ns)] '_125;']);
    eval(['LF_SF_' [pos(ns)] '_Oct(2,' num2str(ii) ')=ELEF_' num2str(ii)...
        '_' [pos(ns)] '_250;']);
    eval(['LF_SF_' [pos(ns)] '_Oct(3,' num2str(ii) ')=ELEF_' num2str(ii)...
        '_' [pos(ns)] '_500;']);
    eval(['LF_SF_' [pos(ns)] '_Oct(4,' num2str(ii) ')=ELEF_' num2str(ii)...
        '_' [pos(ns)] '_1000;']);
    eval(['LF_SF_' [pos(ns)] '_Oct(5,' num2str(ii) ')=ELEF_' num2str(ii)...
        '_' [pos(ns)] '_2000;']);
%          eval(['LF_SF_' [pos(ns)] '_Oct(6,' num2str(ii) ')=ELEF_' ...
%              num2str(ii) '_' [pos(ns)] '_4000;']);
%          eval(['LF_SF_' [pos(ns)] '_Oct(7,' num2str(ii) ')=ELEF_' ...
%              num2str(ii) '_' [pos(ns)] '_8000;']);
end;
end;

end
```

G Appendix 6: *IACC.m*

```
% IACC
%% ----------------------------------------------
clear all
close all
%plot impulse response ?? (1=yes)
plotimp=0;
%%%%%%%%%%%%%%%%%%%%%%%%%%%%%%%%%%%%%%%%%%%%%%%%%%%%%%%%%%%%%
%% -----------  SWEEP   ------------------
fstart=60;       %begin frequency of sweep
fend=20000;      %end frequency of sweep [hz]
T=3;             %time after sweep (for room response)
Fs=44100;        %sampling frequency
[sw, isw] = expsweep(fstart,fend,T,Fs); %sweep
sw=[zeros(44100,1);sw;zeros(44100,1)];  %sweep
t0 = tukeywin(44100*8,0.002);
t1=t0(length(t0)/2:end,1);
t1=[t1;zeros(44100-1,1)];
sw=sw.*t1; %to avoid clip at the end of the sweep

lag=T*44100;          %define length
nges=length(sw)+length(isw)+lag-1;%number of points in fft (fast conv.)

delay=67404;%67412;  % to get the begin of Imp.-Resp. at 1 (latence)


% Measurement with DUMMY HEAD
% delay 1
[imp_KK_1 imp_KK_2 imp_KK_3 imp_KK_4 imp_KK_5 ]=...
    KunstKopf(sw,isw,Fs,lag,nges,delay);
% delay 2
[imp_KK_1_D2 imp_KK_2_D2 imp_KK_3_D2 imp_KK_4_D2 imp_KK_5_D2 ]=...
    KunstKopfD2(sw,isw,Fs,lag,nges,delay);


% 3 octave bands (500, 1k, 2kHz)
[B1,A1] = octdsgn(500,Fs,3);%coeffs for 500Hz oct-band
[B2,A2] = octdsgn(1000,Fs,3);%coeffs for 1kHz oct-band
[B3,A3] = octdsgn(2000,Fs,3);%coeffs for 2kHz oct-band

% DELAY 1
for n=1:5 %rooms
    for o=1:3 %octave band
eval(['left=filter(B' num2str(o) ',A' num2str(o) ',imp_KK_' num2str(n)...
    ');'])
eval(['right=filter(B' num2str(o) ',A' num2str(o) ',imp_KK_' num2str(n)...
    ');'])
eval(['left=left(1:3528,1);'])
eval(['right=right(1:3528,2);'])
a=xcorr(left,right);
b=sqrt(sum(left.^2)*sum(right.^2));
IACF=a/b;
eval(['IACC_0_80(' num2str(n) ',' num2str(o) ')=max(IACF(3528-44:'...
```

```
    '3528+44))'])
    end;
end;

% DELAY 2
for n=1:5
    for o=1:3 %octave band
eval(['left=filter(B' num2str(o) ',A' num2str(o) ',imp_KK_' num2str(n)...
    '_D2);'])
eval(['right=filter(B' num2str(o) ',A' num2str(o) ',imp_KK_' num2str(n)...
    '_D2);'])
eval(['left=left(1:3528,1);'])
eval(['right=right(1:3528,2);'])
a=xcorr(left,right);
b=sqrt(sum(left.^2)*sum(right.^2));
IACF=a/b;
eval(['IACC_0_80_D2(' num2str(n) ',' num2str(o) ')=max(IACF(3528-44:'...
    '3528+44))'])
    end;
end;

% mean values between three octaves
IACC_0_80= mean(IACC_0_80')
IACC_0_80_D2= mean(IACC_0_80_D2')

figure
hold on
plot(1-IACC_0_80)
plot(1-IACC_0_80_D2,'r')
ylabel('1-IACC_{E3}')
set(gca,'XTick', 1:5,'xticklabel',{'Room1','Room2','Room3','Room4',...
    'Room5'});
axis([1,5,0,1])
grid on
legend('Delay 1','Delay 2','Location','Northwest')
```